Effect of carbon substitution on the magnetic properties and crystalline phases of melt-spun $Nd_4Fe_{77.5}B_{18.5}$ alloys

Zhao-hua Cheng, Bao-gen Shen, Fang-wei Wang, Lei Cao, Jian-gao Zhao, and Wen-shan Zhan
State Key Laboratory of Magnetism, Institute of Physics, Chinese Academy of Sciences, Beijing 100080, People's Republic of China

Ming-xi Mao, Ji-jun Sun, Fa-shen Li, and Yi-de Zhang
Department of Physics, University of Lanzhou, Lanzhou 730000, People's Republic of China
(Received 13 July 1994; revised manuscript received 22 December 1994)

The magnetic properties and crystallized phases of melt-spun $Nd_4Fe_{77.5}B_{18.5-x}C_x$ ($x=0$, 4, 6, 8, and 10) alloys have been investigated by means of zero-field spin-echo nuclear magnetic resonance (NMR), x-ray diffraction, and magnetization measurements. The results show that the Curie temperatures of amorphous alloys have a small dependence on carbon concentration, the saturation magnetization of amorphous alloys and the average magnetic moment per Fe atom are found to have a small increase, as x increases from $x=0$ to $x=10$, and, the crystallization temperatures of amorphous alloys decrease with increasing carbon concentration. The amorphous alloys are magnetically soft; their coercive fields are less than 10 Oe. When the ribbons are annealed over the crystallization temperature, the coercivity increases rapidly and reaches a maximum value at the annealing temperature of about 670 °C, then decreases monotonically. Previous studies demonstrated that $Nd_4Fe_{77.5}B_{18.5}$ alloys annealed at 670 °C for a short time consisted only of body-centered-tetragonal Fe_3B (bct Fe_3B) and a few percent of α-Fe. After a short anneal at 670 °C, the coercivity of crystallized alloys decreases with increasing carbon content, with a simultaneous development of an orthorhombic Fe_3B(o-Fe_3B) phase. Furthermore, the NMR study demonstrates that o-Fe_3B has softer magnetic properties than bct Fe_3B. It can be concluded that the addition of carbon in $Nd_4Fe_{77.5}B_{18.5}$ alloy favors the transformation from bct Fe_3B to o-Fe_3(B,C) and the decrease of coercivity is due to the presence of o-Fe_3(B,C).

I. INTRODUCTION

The magnetic properties and crystallization behavior of rapidly quenched Nd-Fe-B with a lower Nd concentration have been extensively investigated for several years.[1-6] After appropriate heat treatments, $Nd_4Fe_{77.5}B_{18.5}$ melt-spun ribbons show a coercivity of 3 kOe, a magnetic remanence of 12.5 kG, and an energy product of 13 MGOe at room temperature.[4] A great deal of work has been performed on the magnetic properties and crystallized phases composition of melt-spun NdFeB alloys because of their practical applications as permanent magnets. However, the detailed phase composition and the origin of hard magnetic properties of crystallized Nd-Fe-B with a low Nd concentration have not been fully understood. In our previous work, a combined spin-echo nuclear magnetic resonance (NMR) and Mössbauer effect (ME) study was undertaken to investigate the phase composition of rapidly quenched $Nd_4Fe_{77.5}B_{18.5}$ alloys annealed under different conditions.[7,8] The effect of Gd substitution on its magnetic properties and hyperfine fields (HF's) was studied as well.[9] The origin of hard magnetic properties was also discussed. It was found that melt-spun $Nd_4Fe_{77.5}B_{18.5}$ alloy annealed at 670 °C did not contain $Nd_2Fe_{14}B$ magnetically hard phase. NMR and Mössbauer spectra demonstrate that the hard magnetic properties originate from body-centered-tetragonal Fe_3B (bct Fe_3B) containing Nd atoms. It is well known that the structural information can be obtained from either diffraction or hyperfine interactions techniques. When the dimensions of some phases are too small to be resolved by x-ray diffraction, or the diffraction patterns for different phases are not easy to distinguish. NMR, one of hyperfine interaction techniques, can be utilized to identify the phase components. The crystallization products are discussed in terms of the known hyperfine parameters of ^{57}Fe and ^{11}B probes in stable and metastable crystalline phases of Fe-B-based alloys. In this work, we present a magnetization measurement and spin-echo NMR study of $Nd_4Fe_{77.5}B_{18.5-x}C_x$ amorphous and crystallized alloys and investigate the effect of carbon substitution on magnetic properties and phase composition.

II. EXPERIMENT

The alloys with nominal composition $Nd_4Fe_{77.5}B_{18.5-x}C_x$ ($0 \le x \le 10$) were prepared via arc melting of iron of 99.9%, neodymium of 99.9%, Fe-B alloy of 98.6%, and Fe-C alloy of 99.8% purity in a high-purity argon atmosphere. The ingots were remelted several times to ensure homogeneity. Amorphous rib-

bons about 1 mm wide and 20 μm thick were prepared by melt spinning at a speed of about 47 m/s. The as-quenched ribbons were heat treated at different temperatures for about 2–300 min in steel capsules evacuated to 2×10^{-5} Torr. An x-ray-diffraction (XRD) experiment was carried out using Co $K\alpha$ radiation. The crystallization and Curie temperatures were determined by a differential scanning calorimeter (DSC) at a scanning rate of 20 K/min and by the temperature dependence of the a.c. susceptibility in a very weak field, respectively. The magnetization curves of amorphous alloys were measured at 1.5 K using an extracting sample magnetometer with a field range 0–70 kOe. The hysteresis loops of the crystallized samples were measured in a vibrating sample magnetometer (VSM) with a maximum magnetic field of 8 kOe. Zero-field spin-echo NMR spectra of ^{11}B and ^{57}Fe were measured at 8 K. The details of NMR measurements have been published elsewhere.[7]

III. RESULTS AND DISCUSSION

A. The Curie temperature and magnetic moment of amorphous alloys

XRD patterns confirm the amorphous state of all as-quenched $Nd_4Fe_{77.5}B_{18.5-x}C_x$ ($0\le x\le10$). Their Curie temperatures T_C as a function of carbon concentration are illustrated in Fig. 1. The T_C of amorphous alloys is found to have a weak dependence on carbon concentration. It is commonly assumed that the T_C of Fe-based alloys is mainly dominated by the Fe-Fe exchange interaction. Substitution of C for B does not have an obvious effect on the Fe-Fe exchange interaction, and hence, the T_C of $Nd_4Fe_{77.5}B_{18.5-x}C_x$ amorphous alloys does not change significantly.

The saturation magnetizations $\sigma_s(1.5)$ at 1.5 K were obtained from fitting the experimental $\sigma(H)$ data versus using the law of approach to saturation. The saturation magnetization as a function of C concentration x is given in Fig. 2. It can be seen that the addition of carbon leads to a small increase in the saturation magnetization. The average magnetic moment $\bar{\mu}_M$ per magnetic atom can be derived from the formula

$$\bar{\mu}_{aM}=\sigma_s(0)M/(N\mu_B)\ , \tag{1}$$

where N is Avogadro's number, μ_B is the Bohr magneton, and M is the molecular weight of the $Nd_4Fe_{77.5}B_{18.5-x}C_x$ alloys. The value of $\sigma_s(0)$ at 0 K is very close to that of $\sigma_s(1.5)$ at 1.5 K. Hence, we can use $\sigma_s(1.5)$ to replace $\sigma_s(0)$.

Because of the ferromagnetic alignment of the effective moment of the ND and Fe atoms, we have

$$\bar{\mu}_M=77.5\bar{\mu}_{Fe}+4\bar{\mu}_{Nd}\ . \tag{2}$$

For the amorphous alloy $Nd_4Fe_{77.5}B_{18.5}$, Nd atomic moments exhibit a noncollinear structure and they are found to be distributed on a cone of half-angle $\Theta=111°$.[10] A previous study demonstrated that the value of Θ was

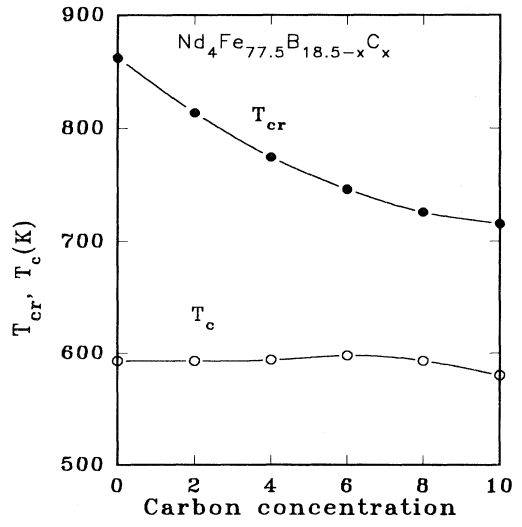

FIG. 1. Curie temperature T_C and crystallization temperature T_{cr} of $Nd_4Fe_{77.5}B_{18.5-x}C_x$ amorphous alloys vs carbon concentration.

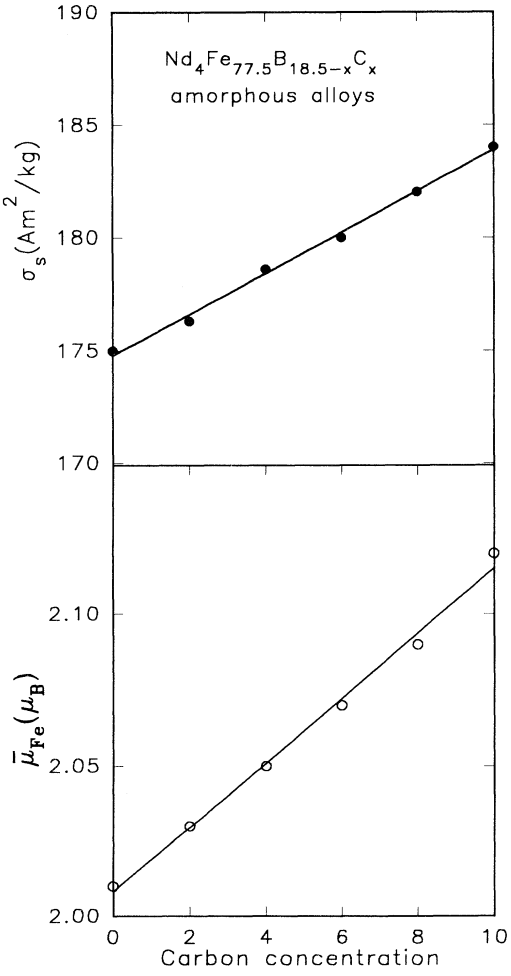

FIG. 2. The saturation magnetization and the average magnetic moment per Fe of $Nd_4Fe_{77.5}B_{18.5-x}C_x$ amorphous alloys as a function of carbon concentration.

slightly influenced by the boron concentration.[11] For amorphous alloys $Nd_4Fe_{77.5}B_{18.5-x}C_x$, the value of Θ is also assumed to be constant for all x on account of the very strong local random anisotropy. From the formula[12]

$$\bar{\mu}_{Nd}=\mu_{Nd}^{3+}(1+\cos\Theta)/2 , \quad (3)$$

where $\mu_{Nd}^{3+}=3.27\mu_B$ is the moment of the free Nd atom, $\bar{\mu}_{Nd}=1.05\mu_B$ can be obtained. So using Eqs. (1) and (2), the concentration dependence of the effective moment per Fe atom $\bar{\mu}_{Fe}$ can be derived, which is shown in Fig. 2. It can be seen that the μ_{Fe} approximately linearly increases from $2.01\mu_B$ to $2.12\mu_B$ for $x=10$. The similar result was also observed in FeBC amorphous allows.[13]

B. The crystallization temperature and phase composition of annealed samples

The crystallization temperatures T_{cr} of amorphous alloys versus carbon concentration x are also presented in Fig. 1. It can be seen from Fig. 1 that T_{cr} decreases monotonically with increasing carbon concentration. This result implies that the addition of carbon atoms reduces the existence range of Nd-Fe-B amorphous alloys. The present work shows that it is very difficult to prepare $Nd_4Fe_{77.5}B_{18.5-x}C_x$ amorphous alloys with $x>10$. Comparing this result with that of Nd,[10] can be found that the Nd and C atoms influence the thermal stability of amorphous alloys in an opposite way. Walter[14] has proposed that in Fe-B alloys substitution of some iron by a larger atom disturbs the close packing, thereby reducing the free volume and the diffusion coefficient. The viscosity of the alloy increases and therefore the thermal stability of the amorphous alloys is enhanced. In the alloys of $Nd_4Fe_{77.5}B_{18.5-x}C_x$, the Nd atoms are larger than the iron atoms, whereas the carbon atoms are smaller than iron atoms. Thus, the contribution of Nd and C to the thermal stability exhibits an opposite behavior.

Melt-spun $Nd_4Fe_{77.5}B_{18.5}$ alloys annealed between 600 and 950 °C produce different crystalline phases. It is found that the samples annealed at temperatures in the range 600–800 °C for a short time show only the metastable bct Fe_3B phase and a few percent of α-Fe; for the sample annealed at 850 °C a paramagnetic phase $Nd_{1.1}Fe_4B_4$ appears in coexistence with bct Fe_3B and α-Fe. The magnetically hard phase $Nd_2Fe_{14}B$ is present only when the annealing temperature is higher than 850 °C, and metastable Fe_3B decomposes to Fe_2B and α-Fe stable phase. The XRD pattern of the sample annealed at 960 °C for 60 min consists of $Nd_2Fe_{14}B$, $Nd_{1.1}Fe_4B_4$, Fe_2B, and α-Fe, as is shown in Fig. 3. Our previous NMR and ME results gave similar results to those of XRD. XRD, NMR, and ME studies show that there is no trace of the remaining amorphous Nd-rich phase in the sample annealed at 670 °C.[7,8] Although previous work assumed that the hard magnetic phase $Nd_2Fe_{14}B$ was present in the sample annealed at 670 °C for a short time, there is a lack of direct evidence. A point of view assumes that the atomic ordering in the $Nd_2Fe_{14}B$ lattice may still be far from perfect and its

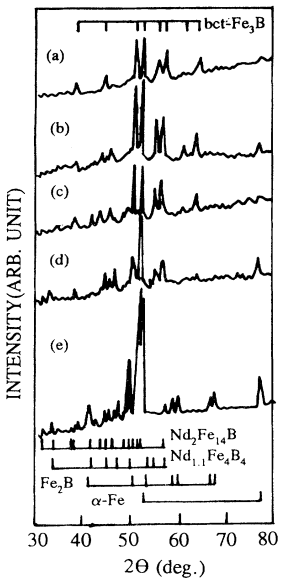

FIG. 3. Co $K\alpha$ radiation x-ray patterns of $Nd_4Fe_{77.5}B_{18.5}$ annealed at (a) 670 °C for 2 min, (b) 670 °C for 300 min, (c) 800 °C for 2 min, (d) 850 °C for 60 min, and (e) 950 °C for 60 min.

grain size is too small to be resolved by XRD, but NMR and ME can identify the phase composition whose dimensions are too small for the XRD technique. Both NMR and ME clearly demonstrated that there was no trace of the $Nd_2Fe_{14}B$ phase presented in this sample. Furthermore, the ^{11}B NMR spectrum shows that the resonance peak broadens asymmetrically to the high frequency and the substitution of Gd for Nd will increase the ^{11}B hyperfine fields in bct Fe_3B;[9] the ME spectrum indicated that the relative intensity of the third subspectrum corresponding to bct Fe_3B is about 5% weaker than those of the other two. On the basis of these results, it is reasonable to assume that some Nd atoms enter into bct Fe_3B lattice in the initial crystallization process due to the imperfection of crystallinity. XRD patterns show that at 670 °C, the annealing time between 2 and 300 min does not influence the phase composition, but only increases the size of crystallite. When the annealing temperature is much higher, Nd atoms from the bct Fe_3B metastable phase form the paramagnetic phase with Fe and B atoms.

The phase components of the carbon-containing alloys annealed under different heat-treated conditions are similar to those of the carbon-free alloy $Nd_4Fe_{77.5}B_{18.5}$. Furthermore, an orthorhombic $Fe_3(B,C)$ (o-Fe_3B) metastable phase coexists with bct Fe_3B in the samples annealed at 600–860 °C. The addition of carbon leads to the formation of an o-Fe_3 (B,C) phase. The samples annealed at 960 °C for 60 min consists of Fe_2B, α-Fe, $Nd_{1.1}Fe_4B_4$, and Nd_2Fe_{14} (B,C) stable phases. The crystallization products of $Nd_4Fe_{77.5}B_{18.5-x}C_x$ annealed at different temperatures are summarized in Table I.

In order to obtain more information concerning the effect of carbon substitution on the formation of o-Fe_3B, we choose the samples annealed at 670 °C for a short

TABLE I. The crystallization products of $Nd_4Fe_{77.5}B_{18.5-x}C_x$ annealed under different heat treatment conditions.

Compounds	670 °C×(2–300 min)	860 °C×60 min	960 °C×60 min
$x=0$	bct $Fe_3B+\alpha$-Fe	bct Fe_3B $+Nd_{1.1}Fe_4B_4$ $+\alpha$-Fe	$Fe_2B+\alpha$-Fe $+Nd_{1.1}Fe_4B_4$ $+Nd_2Fe_{14}B$
$x=2$	bct $Fe_3B+\alpha$-Fe $+o$-Fe_3(B,C)	bct Fe_3B+o-Fe_3(B,C) $+Nd_{1.1}Fe_4B_4$ $+\alpha$-Fe	$Fe_2B+\alpha$-Fe $+Nd_{1.1}Fe_4B_4$ $+Nd_2Fe_{14}$(B,C)
$x=4$	bct $Fe_3B+\alpha$-Fe $+o$-Fe_3(B,C)	bct Fe_3B+o-Fe_3(B,C) $+Nd_{1.1}Fe_4B_4$ $+\alpha$-Fe	$Fe_2B+\alpha$-Fe $+Nd_{1.1}Fe_4B_4$ $+Nd_2Fe_{14}$(B,C)
$x=6$	bct $Fe_3B+\alpha$-Fe $+o$-Fe_3(B,C)	bct Fe_3B+o-Fe_3(B,C) $+Nd_{1.1}Fe_4B_4$ $+\alpha$-Fe	$Fe_2B+\alpha$-Fe $+Nd_{1.1}Fe_4B_4$ $+Nd_2Fe_{14}$(B,C)
$x=8$	bct $Fe_3B+\alpha$-Fe $+o$-Fe_3(B,C)	bct Fe_3B+o-Fe_3(B,C) $+Nd_{1.1}Fe_4B_4$ $+\alpha$-Fe	$Fe_2B+\alpha$-Fe $+Nd_{1.1}Fe_4B_4$ $+Nd_2Fe_{14}$(B,C)
$x=10$	bct $Fe_3B+\alpha$-Fe $+o$-Fe_3(B,C)	bct Fe_3B+o-Fe_3(B,C) $+Nd_{1.1}Fe_4B_4$ $+\alpha$-Fe	$Fe_2B+\alpha$-Fe $+Nd_{1.1}Fe_4B_4$ $+Nd_2Fe_{14}$(B,C)

time, whose phase composition is relatively simple. At this annealing temperature, we investigate the transformation of bct Fe_3B and o-Fe_3B by means of zero-field spin-echo NMR.

Figure 4 shows the ^{11}B and ^{57}Fe spin-echo NMR spectra obtained from the $Nd_4Fe_{77.5}B_{18.5-x}C_x$ ($0\le x\le 10$) alloys annealed at 670 °C. For the sample with $x=0$, the ^{11}B resonance shows a peak centered at 34.7 MHz, which is associated with the ^{11}B nuclei in bct Fe_3B.[15] The NMR study demonstrates that the resonance peak broadens asymmetrically to the high-frequency side. On the basis of previous discussion,[7] this behavior is not attributed to the presence of orthorhombic Fe_3B (o-Fe_3B), but to the entering of Nd atoms into bct Fe_3B phases.[7,8] For the samples with $x>0$, the results clearly show that, in addition to the signal located at 46.7 MHz, which is due to ^{57}Fe nuclei in α-Fe, there are two peaks centered at 34.7 and 36.3 MHz, which are attributed to bct Fe_3B and orthorhombic Fe_3B (o-Fe_3B), respectively,[15] and the latter becomes more distinct with increasing carbon concentration. Since the spin-lattice relaxation time T_1 and the spin-spin relaxation T_2 for various peaks corresponding to bct Fe_3B, o-Fe_3B, and α-Fe, differ from one another, a correction for T_1 and T_2 was taken in plotting Fig. 4. It can be seen that an increase in the carbon concentration causes an increase in the integrate intensity of o-Fe_3B with a corresponding decrease in that of bct Fe_3B peak. The fact that the NMR intensity corresponding to the 36.3-MHz peak increases implies that the addition of carbon favors the transformation from bct Fe_3B to o-Fe_3(B,C). Figure 5 presents the XRD patterns of $Nd_4Fe_{77.5}B_{18.5-x}C_x$ ($x=4$ and 8) annealed at 670 °C for 2 min. The XRD pattern shows bct Fe_3B coexists with o-Fe_3B and α-Fe, the same as the results of NMR. Our previous NMR investigations also demonstrated that the substitution of carbon for boron in Fe-B amorphous alloys can help the formation of o-Fe_3B-like short-range order (SRO).[16] The transformation from bct Fe_3B to o-Fe_3B may be associated with the formation of o-Fe_3B-like SRO in $Nd_4Fe_{77.5}B_{18.5-x}C_x$ amorphous alloys. Only initial crystallization products can reflect the SRO in amorphous materials.

It is well known that NMR can be used to explore the magnetic properties of magnetic materials on the basis of NMR excitation for the nuclei in magnetic materials. In the case of spin-echo NMR experiments, a sequence of two equal-width radio frequency (rf) pulses was used, the optimum rf field for maximum spin-echo intensity is determined by the following expression:[17]

$$\nu\eta_{d,w}h_m\tau=2\pi/3\ , \tag{4}$$

where ν is the gyromagnetic ratio of nuclei measured, τ is the width of rf pulses, $\eta_{d,w}$ is the enhancement factor for domain rotation (η_d) or domain-wall displacement (η_w). For the domain rotation process[18]

$$\eta_d=x_dH_{\rm hf}/M_s\ , \tag{5}$$

while for the domain-wall displacement process

$$\eta_w=x_w(H_{\rm hf}D)/(M_s\delta)\ , \tag{6}$$

where x_d and x_w are the susceptibilities corresponding to domain rotation and domain-wall displacement, respectively, $H_{\rm hf}$ is the hyperfine field at nuclear site, M_s is the

saturation magnetization of the material, D is the size of the domain, and δ is the width of the domain wall. From Eqs. (4)–(6), one can find that the NMR behavior is associated with a parameter reflecting the "easiness" of the magnetization process, i.e., the softer the magnetic properties of the materials, the smaller h_m required to excite the nuclei for a maximum spin-echo signal. Figure 6 shows the spin-echo amplitude corresponding to bct Fe_3B and o-Fe_3B peaks as a function of rf excitation field for $Nd_4Fe_{77.5}B_{10.5}C_8$. It is found that the amplitude of the rf excitation field, h_m, required to get the maximum ^{11}B spin-echo signal from the o-Fe_3B phases (36.3 MHz) is only about one-fourth as much as that required for exciting the ^{11}B NMR signal in the bct Fe_3B (34.7 MHz). Thus, it can be concluded that the o-Fe_3B phases have a larger n_w, and hence, are more easily magnetized than the bct Fe_3B phases. That is to say, the coercivity of the o-Fe_3B phase is smaller than that of bct Fe_3B. Since a pure o-Fe_3B phase sample has not been fabricated until now, it is impossible to compare the bulk magnetic properties of the bct Fe_3B and o-Fe_3B phases directly; the present NMR results shown in Fig. 6, however, make a comparison possible. Magnetization measurements indi-

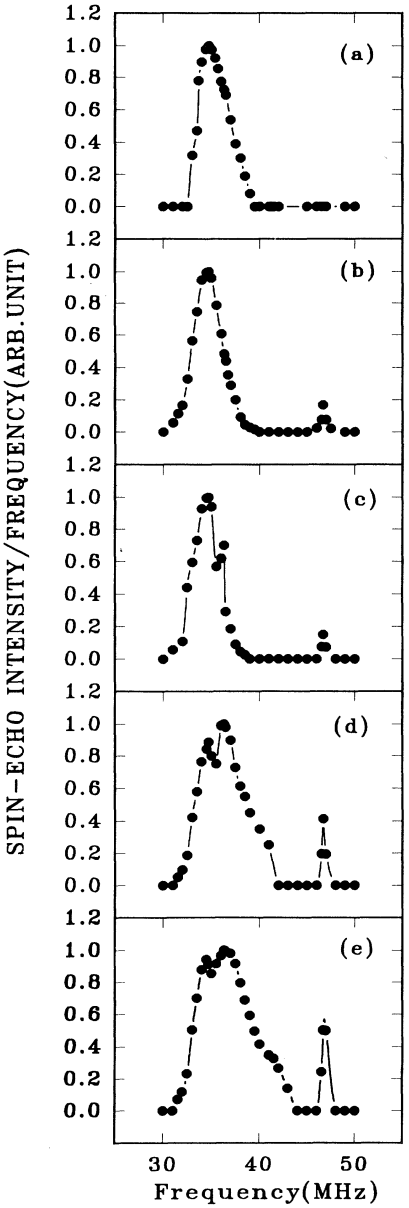

FIG. 4. Spin-echo NMR spectra of $Nd_4Fe_{77.5}B_{18.5-x}C_x$ alloys annealed at 670 °C for a short time, (a) $x=0$, (b) $x=4$, (c) $x=6$, (d) $x=8$, and (e) $x=10$.

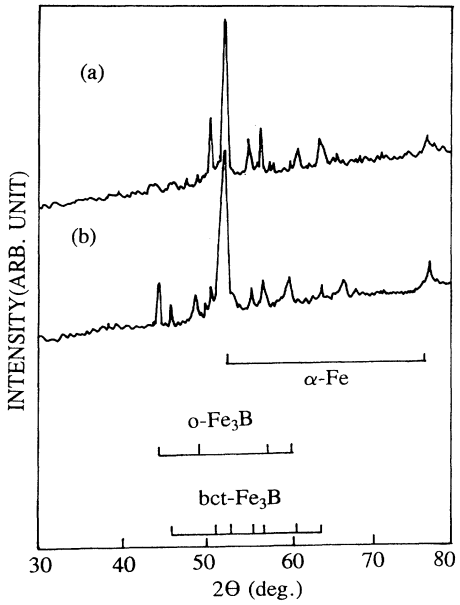

FIG. 5. Co $K\alpha$ radiation x-ray patterns of $Nd_4Fe_{77.5}B_{14.5}C_4$ (a) and $Nd_4Fe_{77.5}B_{10.5}C_8$ (b) annealed at 670 °C for 2 min.

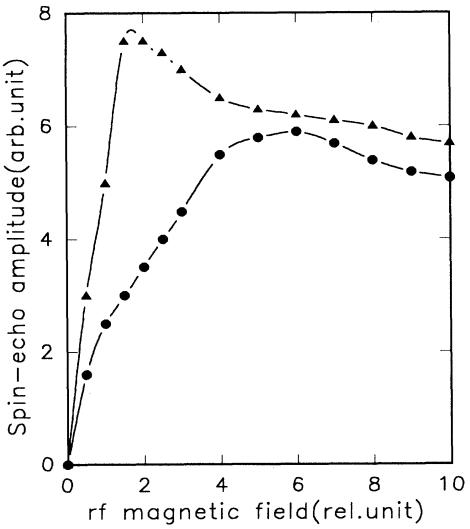

FIG. 6. The ^{11}B spin-echo NMR signal amplitude corresponding to bct Fe_3B and o-Fe_3B peaks as a function of rf excitation field for $Nd_4Fe_{77.5}B_{10.6}C_8$: solid circles, peak at 34.7 MHz (bct Fe_3B); solid triangles, peak at 36.3 MHz (o-Fe_3B).

cate the coercivity of these crystallized alloys decreases rapidly from 3 kOe for $x=0$ to about 50 Oe for $x=10$. Thus, the sharp decrease of coercivity is not only due to the increase of α-Fe concentration, but also to the presence of o-$Fe_3(B,C)$.

IV. CONCLUSION

(1) The addition of carbon atoms leads to an increase in the average magnetic moment per Fe atom and to a monotonous decrease in the crystallization temperature of amorphous alloys. However, their Curie temperatures are nearly independent of carbon concentration.

(2) There are two types of Fe_3B phases in carbon-containing crystallized allows: o-Fe_3B and bct Fe_3B. The substitution of carbon for boron atoms favors the formation of o-Fe_3B phase.

(3) The presence of the o-Fe_3B phase results in a lower coercivity than bct Fe_3B and the decrease of coercivity is attributed to the replacement of the bct Fe_3B phase by o-Fe_3B ones.

ACKNOWLEDGMENT

This work was supported by the National Natural Sciences Foundation of China and State Key Laboratory of Magnetism, Institute of Physics, Chinese Academy of Sciences.

[1]R. Coehoorn, D. B. de Mooij, J. P. Duchateau, and K. H. J. Buschow, J. Phys. (Paris) Colloq. **49**, C8-669 (1988).

[2]R. Coehoorn and C. de Waard, J. Magn. Magn. Mater. **83**, 228 (1990).

[3]K. H. J. Buschow, D. B. de Mooij, and R. Coehoorn, J. Less-Common Met. **145**, 601 (1988).

[4]B. G. Shen, J. X. Zhang, L. Y. Yang, F. Wo, T. S. Ning, S. Q. Ji, J. G. Zhao, H. Q. Guo, and W. S. Zhan, J. Magn. Magn. Mater. **89**, 195 (1990).

[5]K. H. Müller, J. Schneider, H. Handestein, D. Eckert, and P. Nothnagel, Mater. Sci. Eng. A **133**, 151 (1991).

[6]B. G. Shen, L. Y. Yang, J. Z. Liang, and H. Q. Guo, J. Phys. Condens. Matter **4**, 7247 (1992).

[7]M. X. Mao, C. L. Yang, Z. H. Cheng, Y. D. Zhang, B. G. Shen, L. Y. Yang, and F. S. Li, J. Phys. Condens. Matter **4**, 9147 (1992).

[8]M. X. Mao, Z. H. Cheng, C. L. Yang, F. S. Li, C. L. Zhang, Y. D. Zhang, B. G. Shen, and L. Y. Yang, J. Appl. Phys. **73**, 6980 (1993).

[9]Z. H. Cheng, M. X. Mao, J. J. Sun, B. G. Shen, C. L. Yang, F. S. Li, and Y. D. Zhang, J. Phys. Condens. Matter **6**, 7437 (1994).

[10]B. G. Shen, J. X. Zhang, L. Y. Yang, H. Q. Guo, and J. G. Zhao, Mater. Sci. Eng. A **133**, 162 (1991).

[11]*Proceedings of the International Conference on Rare Earth Developments and Applications,* edited by J. G. Zhao, B. G. Shen, W. S. Zhan, G. X. Xu, and J. M. Xiao (Sciences Press, Beijing, 1985), p. 895.

[12]J. M. D. Coey, J. Chappert, J. P. Rebouillat, and T. S. Wang, Phys. Rev. Lett. **36**, 1061 (1976).

[13]F. Z. Luborsky, J. J. Becker, J. L. Walter, and D. L. Martin, IEEE Trans. Magn. **Mag-16**, 521 (1980).

[14]J. L. Walter, Mater. Sci. Eng. **50**, 137 (1981).

[15]Y. D. Zhang, J. I. Budnick, J. C. Ford, and W. A. Hines, J. Magn. Magn. Mater. **100**, 13 (1991).

[16]S. H. Ge, M. X. Mao, G. L. Chen, Z. H. Cheng, C. L. Zhang, W. A. Hines, and J. I. Budnick, Phys. Rev. B **45**, 4695 (1992).

[17]W. B. Mims, Phys. Rev. **141**, 499 (1966).

[18]A. V. Zalesskij and I. S. Zheludev, At. Energy. Rev. **14**, 133 (1976).